



Research paper

Comparative design space exploration of centred and off-centred semisubmersible configurations for floating offshore wind turbines

Claudio A. Rodríguez Castillo^{a,b,*}, Maurizio Collu^a, Feargal Brennan^a

^a Department of Naval Architecture, Ocean & Marine Engineering, University of Strathclyde, 100 Montrose St, Glasgow, G4 0LZ, United Kingdom

^b Department of Naval and Ocean Engineering, Federal University of Rio de Janeiro, Av. Athos Silveira, 149 - CT, Bloco C, Sala 203, Cidade Universitária, Rio de Janeiro, CEP 21.945-97, RJ, Brazil

ARTICLE INFO

Keywords:

Floating substructure
Floating platform
Hull optimisation
Ocean renewable energy
Marine hydrodynamics

ABSTRACT

Achieving net-zero carbon goals demands an accelerated energy transition, with offshore wind energy emerging as a key contributor due to its vast potential. While floating offshore wind turbines (FOWTs) have seen significant progress through demonstrators, scaling up turbine capacities and deploying large-scale wind farms require further research and innovation. This study explores the design trade-offs between centred and off-centred semisubmersible configurations in FOWTs, using the UMaine and WindFloat designs as base for representative case studies. Parametric analyses were conducted to evaluate key aspects such as dimensioning, mass properties, equilibrium, intact stability, natural periods, and wave-induced loads, applied to the 15-MW IEA reference wind turbine at Scotland's NE8 offshore site. The findings reveal that off-centred semisubmersible configurations face significant challenges due to stringent ballast distribution constraints, which restrict the feasible design space. Conversely, centred semisubmersible configurations demonstrated better overall performance across key design metrics, achieving these outcomes with notably less hull steel mass. These results highlight the critical influence of tower placement on floating substructure design, emphasising the importance of refining and optimising proven configurations to support the development of efficient, large-scale floating wind energy systems.

1. Introduction

As the demand for renewable energy grows, wind energy harnessing is pushed further offshore and into deeper waters, requiring floating substructures as cost-effective solutions. So far, few concepts have demonstrated their technical feasibility in full-scale projects such as Hywind (Equinor, 2024) and Kincardine (Flotation-Energy, 2024), based on spar and semisubmersible floating substructures, respectively. Other concepts, such as barge or TLP, have also been proposed but in terms of number of deployed units, wind power capacity, and Technological Readiness Level (TRL) (Proskovics, 2018), they are not yet at the same level of the other platform types. A recent comprehensive review by (Edwards et al., 2024) examines the trends in floating offshore wind platform designs. The study identifies and classifies 86 early-stage floating offshore wind turbine (FOWT) platform designs along a four-phase evolutionary timeline. It highlights the industry's progression from oil and gas (O&G)-inspired concepts to purpose-built FOWT designs. The current phase (Phase IV) is marked by a strong focus on cost

reduction as the primary design driver. Indeed, the floating platform (including mooring) can represent over 50% of the manufacturing costs of a FOWT, with the semisubmersible being the cheapest option compared to a spar or a TLP (Castro-Santos and Diaz-Casas, 2014). Furthermore, the floating platform has a direct influence on the tower top motions, which are closely correlated to the wind turbine performance and the generated power. Then, since the motions of FOWTs are basically dependant on the geometry of its floating substructure, its optimisation is of paramount importance because it could lead to a significant reduction in cost. In terms of farm scale, according to (Edwards et al., 2024), cost reduction has faced a challenging compromise between developing standardised and site-dedicated designs, which is reflected in the recent divergence in floating platform designs, especially of the semisubmersible type, as, for instance, Tri-Floater (NOV, 2024), D-Floater and T-Floater (BT. BT Floater Design, 2024), Deepsea Star (odfjell-oceanwind, 2024), BRUNEL (Dos Santos et al., 2024; Fred Olsen 1848, 2024), XCF (Mareal. XCF, 2024), Y-shaped semi (Li et al., 2022), JMU's design (Matsuoka et al., 2022), Trivane (2022),

* Corresponding author. NAOME, University of Strathclyde, 100 Montrose St, Glasgow, G4 0LZ, United Kingdom.

E-mail addresses: claudiorc@oceanica.ufrj.br, claudio.rodriguez-castillo@strath.ac.uk (C.A. Rodríguez Castillo), maurizio.collu@strath.ac.uk (M. Collu), feargal.brennan@strath.ac.uk (F. Brennan).

<https://doi.org/10.1016/j.oceaneng.2025.120740>

Received 4 December 2024; Received in revised form 11 February 2025; Accepted 18 February 2025

Available online 22 February 2025

0029-8018/© 2025 The Authors. Published by Elsevier Ltd. This is an open access article under the CC BY license (<http://creativecommons.org/licenses/by/4.0/>).

ActiveFloat (Mahfouz et al., 2021), WINDMOOR (Silva de Souza et al., 2021), among others (Edwards et al., 2023a, 2023b). Indeed, each of those designs may have specific, unique characteristics, but many of them share basic features. For instance, it is possible to identify a category of semisubmersibles which have three columns connected with bracings, with heave plates, most likely influenced by the successful WindFloat demonstrator (Roddier et al., 2017). In this subcategory, the tower that supports the wind turbine is located on the external perimeter of the platform, to reduce the required crane's reach during the assembly of the FOWT. A second category is represented by braceless floating substructures with pontoons (Allen et al., 2020; Luan, 2018), with three external columns and a central one that supports the tower. This category aims at avoiding manufacturing complexities and fatigue related issues in the joints between bracings and columns. Finally, a third category includes all the floating substructures not covered by and/or divert further from the "more established" previous categories, such as those using four or more external columns (Fenu et al., 2020; Matsuoka et al., 2022; Yang et al., 2022).

The complexity and multidisciplinary characteristics of FOWT systems, also due to the several configurations proposed, has led to a growing interest in optimisation techniques, particularly those focused on multi-objective optimisation. Although the concept of multidisciplinary design, analysis, and optimisation (MDAO) is widely applied in aerospace and automotive industries, it is still at its infancy in the FOWT sector (Ojo et al., 2022). Recent comprehensive review studies on multi-objective optimisation techniques applied to the design of floating substructures for FOWT can be found in (Ojo et al., 2022; Patryniak et al., 2022; Sykes et al., 2023). Those reviews indicate that the majority of studies focus on FOWTs with capacities in the lower 5–10 MW range, primarily utilising spar-type floating substructures. This preference is likely due to the simple geometry of spar designs, which facilitates easier implementation and analysis. A few works have focused on the comparison of different types of floating substructures such as in (Karimi et al., 2017) or (Ghigo et al., 2020), where semisubmersibles, spars, and TLP designs are investigated, while even less works can be found specifically on semisubmersibles such as in (Lemmer et al., 2020; Ferri et al., 2022) or (Zhou et al., 2023). Furthermore, most of the semisubmersible designs, investigated in design space exploration or optimisation works, are either based on the OC4 reference design (Robertson et al., 2014), or on conceptual designs that have still not progressed into full-scale demonstrator phase – evidencing not only the trend to divergence pointed out by (Edwards et al., 2024), but also a certain mismatch between academic research and the trend observed among industry designers. Indeed, in order to increase the design space of the FOWT substructures, some research works suggest deviating from traditional geometric shapes (Patryniak et al., 2022) and/or adopt ship hull curve parametrisation techniques such as B-spline or free-form deformation (Ojo et al., 2022). Certainly, under the perspective of economy of scales and cost reduction, within larger and more comprehensive design spaces and optimisation frameworks, it is likely to find better design solutions than those currently deployed and extensively investigated. However, they may not be necessarily the optimal ones in terms of whole life-cycle assessment or in terms of time to delivery. In the context of accelerating the energy transition, the latter aspect is crucial.

Being aware of the paramount importance of optimising floating platform designs for FOWTs, but avoiding the divergence in design concepts, this study investigates two of the most representative semisubmersible categories: the off-centred (tower) configuration, exemplified by WindFloat design (by Principle Power), and the centred (tower) configuration, characterised by VoltturnUS UMaine design (by UMaine and NREL). These configurations will be aligned with the current industry focus on turbines capacities of 15-MW and above (Sykes et al., 2023). The off-centred semisubmersible configuration, featured by its offset tower placement has been extensively investigated by their developers and partners at model scale, and with demonstrators deployed at sea in Portugal (Roddier et al., 2017) and Scotland (Flotation-Energy,

2024). It is often praised for its ability to minimise crane outreach during turbine installation and commissioning at quayside (Principle-Power, 2024), although it comes at the cost of uneven weight distribution of the ballast in the FOWT. The centred semisubmersible configuration, on the other hand, incorporates a central column to directly support the tower, providing a more symmetric weight (and ballast) distribution. This design has also been extensively investigated, both numerically and experimentally, by developers and independent researchers, including the deployment of a demonstrator in the United States (Viselli et al., 2016).

Both semisubmersible configurations feature three external columns but differ in key hull components. The off-centred design employs bracings and heave plates to enhance motion response performance, while the centred design adopts an additional (central) column to support the tower and pontoons in Y-configuration to connect the columns. Despite their widespread adoption and ongoing development, there is a notable gap in the literature regarding a detailed comparative analysis of these designs and their fundamental performance characteristics.

To address this gap, the present work parametrises and implements these semisubmersible configurations using an in-house computational tool. This tool systematically explores the design space of the main geometrical parameters and computes hydrostatics, hull steel mass and inertia, equilibrium and ballast conditions, stability, free-floating natural periods, and wave-induced loads. These calculations are performed following naval architecture principles in modular framework, enabling efficient and comprehensive design space exploration.

The study aims at bridging the gap in the understanding of global response characteristics of FOWT semisubmersible platforms (Li et al., 2024), focusing on the two most representative configurations. Moreover, the methodology proposed could serve as a prefiltering tool (of the design space) within a multidisciplinary optimisation procedure, as suggested by (Sykes et al., 2023). By ensuring that only floating substructures that have satisfied equilibrium, stability, and hydrodynamic criteria advance to more complex and computationally demanding simulations, this approach has the potential to streamline the design process and enhance overall efficiency.

2. Methods and materials

2.1. Design methodology

According to (Li et al., 2024), the design of a FOWT platform is an iterative process that can be divided in three design phases. The first phase covers the rationale, the criteria and the selection of the floater concept and its subtype, the second phase involves the determination of global dimensions (diameters, lengths, heights, distances, etc.) for the chosen subtype, and the third phase focuses on the detailed structural design, to determine floating substructure scantlings based on ultimate limit state (ULS) and fatigue limit state (FLS) checks. In theory, the "optimal" design is obtained after several iterations across the three design phases, for every floater concept and subtype. However, in practice, that iterative procedure encompassing such a broad scope may not be computationally practical and efficient. On the other hand, recently (Li et al., 2024) have proposed a simplified approach, denominated global design methodology, where the selection of the concept and its subtype is not part of the overall design iterative process, but instead involves a judgement based on given factors such as the characteristics of the offshore site (water depth, geotechnics, environmental conditions) and the wind turbine properties, and the designer criteria based on expertise, research studies, industry practises, etc. Once the concept and the subtype of the floating platform is selected, its global (main) dimensions will be obtained based on sensitivity studies and global design criteria, such as serviceability, intact stability, and motion natural periods.

Since the global design methodology fits well to the premises and scope of the present work, it will be used as a basis for the design space

exploration here proposed.

2.2. Premises and criteria

The review conducted and reported in the Introduction section has evidenced that the semisubmersible is the most popular floating platform concept for FOWTs, being the centred and off-centred tower configurations, the most preferred subtypes. In the context of the global design methodology, each subtype is assessed separately but using the same offshore site and wind turbine as given inputs. The choice of the wind turbine constraints the mass properties and performance characteristics of the Rotor-Nacelle assembly (RNA), as well as the tower main dimensions and mass properties. In reality, the tower for a FOWT is a design problem itself and has specific challenges, particularly in terms of modes of vibration and their frequencies, as well as tower fatigue, which in turn are heavily influenced by the platform characteristics, but these aspects are out of the scope of the present work since the main focus is on the floating substructure and not the tower. The line pretensions and fairlead locations of the mooring system are also required for the preliminary design and will be also assumed as given inputs.

During the parametric studies, each of the design candidates will be assessed in terms of hydrostatics (equilibrium and ballasting) and stability, hydrodynamics (motion natural periods and wave excitation loads), and cost (bill of material estimates).

2.2.1. Hydrostatics & stability

Equilibrium is assessed in terms of feasibility of the required ballast mass and distribution to achieve a specified draught. Intact stability is evaluated based on the static angle resulting from the application of the heeling moment induced by the maximum mean thrust of the wind turbine and the righting moment (RM) of the floating platform, which is given by (Lewis, 1988):

$$RM = [\rho g I + (\rho g \nabla KB - mgKG)]\theta \approx \rho g \nabla GM\theta \quad (1)$$

with:

$$BM = \frac{I}{\nabla}; \quad KM = KB + BM; \quad GM = KM - KG; \quad (2)$$

where: ρ and g are the water density and gravity acceleration, respectively; I is the second moment of area of the waterplane with respect to (wrt) the inclination axis considered, ∇ is the displaced volume of the platform, KB the vertical centre of buoyancy wrt the platform's keel, m is the mass of the FOWT system, KG is vertical position of the centre of gravity wrt platform's keel, BM is the metacentric radius, KM is the height of the metacentre wrt the keel, and GM is the metacentric height. Eq. (1) assumes small inclination angles (θ) and negligible effect of the inclination moment induced by the mooring system. The resultant static angle is deemed as a serviceability criterion for FOWTs where typically a threshold in the range of 5–10° is adopted (DNV, 2021a; Ferri et al., 2022; Ghigo et al., 2020; Karimi et al., 2017; Li et al., 2024; Wayman, 2006; Zhou et al., 2023).

2.2.2. Hydrodynamics

Usually, hydrodynamic performance of the FOWTs is assessed in terms of motions or response amplitudes. To reliably predict platform responses, all the loads should be known, which is not the case in early design stages. Furthermore, the prediction of those loads is typically challenging, especially, those related to hydrodynamics. Thus, usually approximations or simplifying premises are adopted, such as potential flow theory where, for instance, viscosity is neglected. Since viscous effects may play a significant role in motion prediction, usually viscous loads are introduced by assuming pre-specified damping/drag contributions. The latter, however, may involve large uncertainties, which have an impact on motions predictions.

An alternative approach to assess the hydrodynamic performance is

to determine the system's natural periods of motions so that certain ranges of loads excitation periods are avoided. For FOWTs the main dynamic excitation loads come from waves and wind, with rotor speed harmonics (especially 1P and 3P) being of particular relevance for tower design and tension-leg platforms (TLPs). In terms of excitation periods of the floating substructure, dynamic wind loads are typically more relevant for surge, sway, and yaw (mooring induced) natural periods, while wave loads are of concern for heave, roll and pitch natural periods – at least, in the context of first order (linear) wave loads. Since the mooring system is out of the scope of the present work, only heave and pitch (or roll) natural periods will be verified using the decoupled, single-degree-of-freedom, rigid-body approach, i.e.:

$$T_{n3} = 2\pi \left(\frac{m + A_{33}}{\rho g A_{WP}} \right)^{1/2} \quad (3)$$

$$T_{n5} = 2\pi \left(\frac{J_{yy} + A_{55}}{mgGM} \right)^{1/2} \quad (4)$$

where: m represents the overall system's mass, A_{WP} is the waterplane area, and A_{33} and A_{55} are the added mass and inertia coefficients in heave and pitch, respectively. Added mass coefficient usually requires the numerical solution of a radiation three-dimensional boundary value problem of involving panel mesh solvers such as Wamit® (Lee and Newman, 2013). Although some Authors have used that approach in a few optimisation studies (Ferri et al., 2022; Karimi et al., 2017), due to its relatively high computational effort, it may not be practical for preliminary design stages, where large design spaces need to be explored. Since the geometries of the off-centred and centred configurations can be decomposed in simple geometrical bodies such as cylinders, square prisms, discs, and others, the analytical expressions provided in (DNV, 2021b) can be used for the calculation of added mass coefficients. This approach assumes that the bodies are in infinite fluid (far from boundaries), i.e., frequency independent, but it is efficient and sufficiently accurate for preliminary design purposes. Typically, the motion natural periods of heave (T_{n3}) and pitch (T_{n5}) are usually constrained by, respectively, $T_{n3} > 17\text{--}20$ s and $T_{n5} > 20\text{--}25$ s (Li et al., 2024; Zhou et al., 2023) to avoid resonance with the most energetic wave components of the seas at the offshore site.

The computation of wave-induced loads on semisubmersibles is typically performed within the numerical solution of a 3D radiation-diffraction boundary value problem, which involves meshing the surface of the floating platform using panels. Indeed, several studies on FOWTs rely on medium-to-high fidelity hydrodynamic modelling tools, such as Sesam HydroD (Li et al., 2024), or Wamit (Ferri et al., 2022; Karimi et al., 2017). However, in the context of an early design stage, where large sets ($\sim 10^3$) of floating substructures need to be analysed, the use of panels methods may not be suitable due its computational cost.

On the other hand, based on the premise that for sufficiently long waves (compared to body characteristic dimensions), the scattering (or diffraction) component of the wave-excitation load has a secondary (or even negligible) contribution, the Froude-Krylov (FK) component can be used here to represent the total wave-induced forces and moments. The (undisturbed or FK) wave-induced pressure field by a regular wave of amplitude ζ_a and frequency ω , is given by:

$$p^{(FK)} = \rho g \zeta_a \frac{\cos h[k(z+d)]}{\cos h(kd)} \cos(kx \cos \beta + ky \sin \beta - \omega t) \quad (5)$$

where k is the wave number, d is water depth, β is the angle of wave incidence ($\beta = 0^\circ$ for waves following the positive x-direction of the global reference frame), t is time, and (x, y, z) represent the coordinates of each point on the floating substructure surface. Since most of the typical floating substructure of FOWTs can be decomposed in simple geometries (e.g., cylinders, parallelepipeds, disks, etc.) described by

analytical expressions, the computation of (FK) wave excitation loads can also be performed analytically, substantially reducing computational times. Although this approach disregards the scattering (diffraction) loads – important for large volume structures such as semisubmersibles – it captures the trends and most representative contributions of the wave excitation, particularly for longer waves – typical of extreme sea states.

For the hull geometries considered in this study, heave and pitch FK loads can be computed analytically (and exactly), eliminating the need for panel-method-based software which are time-prohibitive for wide-ranging design space exploration. The FK approach proposed here offers a novel and efficient method for the preliminary parametric analysis of FOWT floating substructures. Its simplicity and computational efficiency make it particularly suitable for comparative studies across a broad design space, paving the way for faster and more accessible design optimisation.

In summary, from the Authors’ perspective, the assessment of the floating platform dynamics of FOWTs, based on wave excitation loads and motion natural periods constraints, involves less uncertainties and may provide a more reliable picture of the design space when compared to the dynamics assessment based on wave-induced motion responses such as in (Ferri et al., 2022; Karimi et al., 2017; Zhou et al., 2023). Since the latter generally involves arbitrary assumptions related to viscous damping loads (which strongly affect resonant amplitudes) especially when comparing different floating substructure geometries, potential distortions of the design space could be introduced due to under or overestimation of response amplitudes.

2.2.3. Cost

Bill of material (and potentially, also wave excitation loads) could be deemed as objective functions aimed at being minimised, provided that equilibrium, stability, and motion periods criteria are satisfied. Bill of material will be indirectly assessed by means of hull steel mass. The computation of hull steel mass is related to the internal structure (scantlings) of the floating platform, including thicknesses determination, but these can only be specified in the detailed design stage (phase

3). For the preliminary design stages of FOWTs, a single equivalent plate thickness is usually adopted as representative of the overall internal floating substructure structure (Lemmer et al., 2020; Li et al., 2022, 2024; Yang et al., 2022; Zhou et al., 2023).

The aforementioned design aspects have been organised in modules and implemented numerically in an in-house code, to allow for an efficient subsequent parametric analysis. In Fig. 1 the modules are illustrated within dashed box contours, with the arrows showing the flux of data from the input module and within the functions performed in each module.

2.3. Parametric analysis (high-level optimisation)

The design space exploration was performed using a parametric analysis approach, focusing on the global dimensions of the floating platform. After selecting the semisubmersible configuration, the floating substructure was parametrised using a set of primary dimensions (design variables or design vector). These primary dimensions serve as the basis for deriving all the other (secondary) dimensions through geometric relationships, established from a reference floating substructure geometry. For the off-centred semisubmersible configuration, the geometric relationships were derived from several published works, including (ABS, 2021; Banister, 2017; Cermelli et al., 2009; Principle. WindFloat Pacific OSW Project, 2014). Similarly, for the centred configuration, the reference geometry was based on the VoltornUS UMaine semisubmersible reported by (Allen et al., 2020). The primary geometrical parameters of each semisubmersible configuration are displayed in Fig. 2. In this figure, D represents the external column diameter, R the radius of the array of the external columns, d_c is the central column diameter, T is the design (operational) draught and f_b is the freeboard.

The number of free design variables can, in theory, be as large as desired. However, an excessive number of variables may lead to impractical designs and inefficient exploration of the design space. Therefore, it is recommended to minimise the number of primary parameters by employing principles of geometrical similarity, as well as designer’s expertise and criteria, while retaining sufficient flexibility to

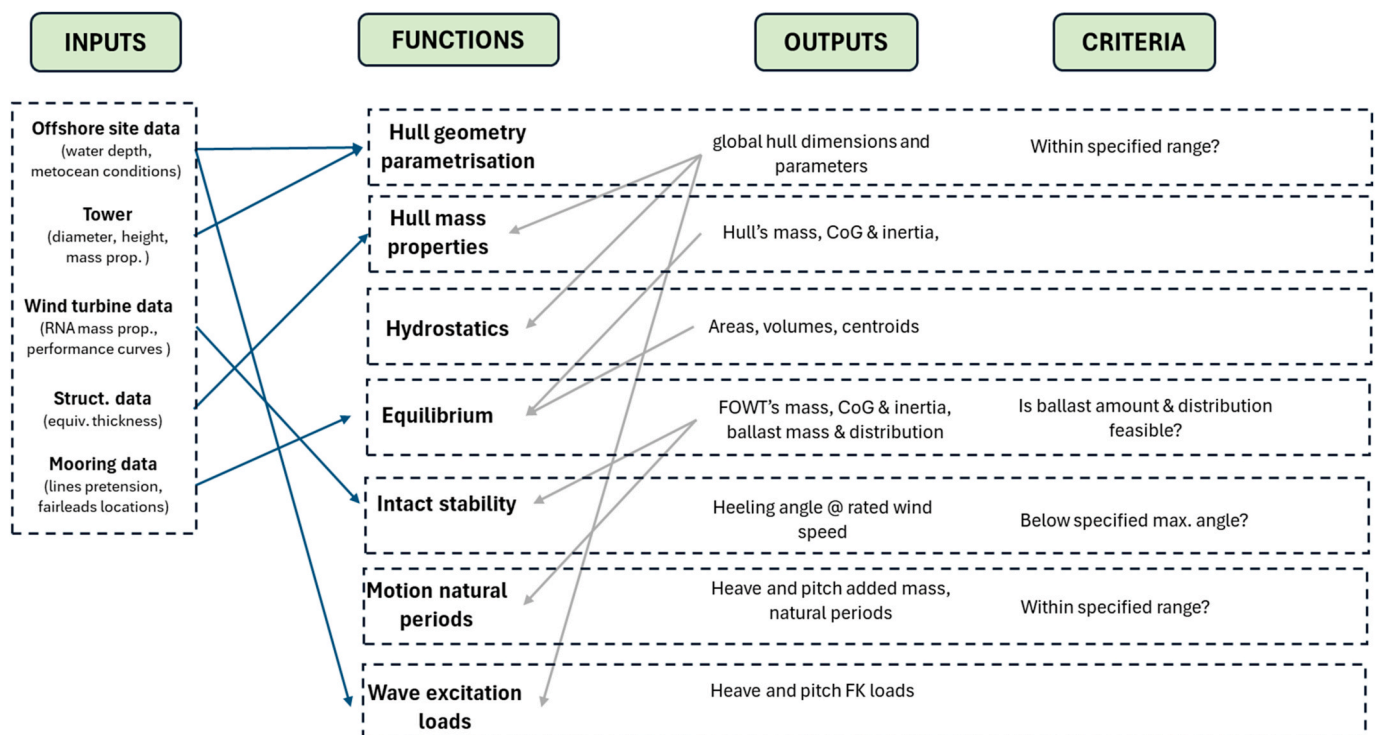


Fig. 1. Modules and flux of data adopted for design assessment.

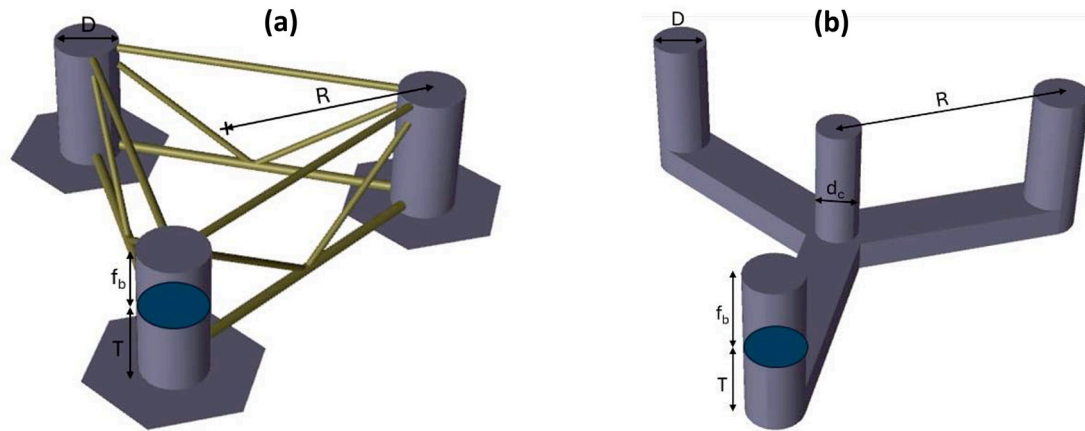


Fig. 2. Primary geometrical parameters of the semisubmersible configurations: (a) off-centred, (b) centred.

explore relevant domains of the design space. For instance, in the centred configuration analysed here, the pontoon width is assumed to equal the diameter of the external columns – aiming at ease of construction and assembly. Additionally, the pontoon height is defined as a fraction of the operational draught – avoiding unnecessary proximity to the free surface and the associated increased hydrodynamic loads. Moreover, although the central column diameter is considered a free variable, it is assumed to match the tower base diameter. The latter results from the tower design, assumed here as input data.

Once the primary geometric parameters are established, variation ranges are assigned to each parameter. These ranges are systematically combined in pairs, with all other parameters held constant, allowing for a comprehensive exploration of thousands of potential floating substructure geometries. For each configuration, mass properties, hydrostatics, equilibrium, and stability characteristics are calculated, and verified against the stability criterion associated to the wind-induced heeling angle at rated wind speed (also referred to as serviceability criterion in (Li et al., 2024)). Only configurations meeting this criterion proceed to have their natural periods and wave excitation loads evaluated. The resulting reduced design space can then be reviewed to identify the most promising floating substructure geometries.

3. Case study: 15 MW wind-turbine

The proposed procedure described in Section 2 will be used to explore the design space of the centred and the off-centred semisubmersible configurations, using as case study a 15-MW wind turbine. Due to its open-accessibility and detailed information, the IEA reference 15-MW wind turbine reported in (Gaertner et al., 2020) will be adopted. Other relevant design parameters, such as baseline values for the floating substructure geometry, tower, and mooring system properties will be taken from the reference VoltturnUS UMaine semisubmersible reported in (Allen et al., 2020). Table 1 summarises the input data used as design specifications (requirements) for the parametric analyses of both semisubmersible designs. The ScotWind Lease area NE8 (Crown-State-Scotland, 2021), planned for a 1-GW floating wind farm, was considered as representative offshore site. The metocean data for that site were obtained from the EU ERA5 Reanalysis database (Hersbach et al., 2023). The water depth for that region ranges between 100 and 200 m, but 200 m will be assumed so that the same mooring system of the reference UMaine platform can be used. The equivalent plate thickness was obtained following an iterative procedure that aimed at matching the floating substructure steel mass of the reference UMaine semisubmersible. The same equivalent thickness (45.4 mm) will be adopted for all the investigated off-centred and centred semisubmersible configurations. That value seems to be in agreement with equivalent plate thicknesses reported in the literature for other

Table 1
Input data (specifications).

Description	Units	Values
Wind turbine data		
Power rating	MW	15.0
Rotor thrust @ rated wind speed	kN	2445.4
Hub height	m	150.0
Nacelle mass	t	675.2
Nacelle CoG	m	(-4.528, 0.140, 148.484)
Nacelle inertia	t.m ²	(9.913E+03, 1.086E+04, 1.036E+04)
Rotor mass (inc. hub)	t	274.9
Rotor CoG (inc. hub)	m	(-13.644, 0.0, 150.170)
Rotor inertia (inc. hub)	t.m ²	(1.751E+05, 1.751E+05, 3.468E+05)
Tower data		
Tower base diameter	m	10.0
z_tower base	m	15.0
z_tower top	m	144.4
Tower mass	t	1483.1
Tower CoG	m	(0.0, 0.0, 56.68)
Tower inertia	t.m ²	(1.356E+06, 1.356E+06, 3.646E+04)
Tower drag @ rated wind speed	kN	72.4
z_tower drag @ rated wind speed	m	85.3
Structural data		
Equivalent hull thickness	m	0.045
Mooring system data		
Fairlead pretension	kN	7311.0
Fairlead angle from SWL	deg	56.4
z_fairlead	m	-14.0
Offshore site data (NE8)		
Water depth	m	200.0
50-y significant wave height	m	11.08
50-y wave peak period	s	13.71
JONSWAP peak-enhancement factor	-	2.75

CoG: Centre of Gravity; x, y coordinates wrt tower centre, z wrt still water level (SWL), inertias wrt local CoG.

semisubmersible optimisation studies, where typical values are 35.6 mm (Zhou et al., 2023), 45 mm (Li et al., 2022), 50 mm (Karimi et al., 2017; Li et al., 2024) or 60 mm (Yang et al., 2022).

The design variables, baseline values, and ranges of variation used for the parametric analyses are summarised in Table 2. Since the parameters that have the most significant influence are the column centreline spacing (defined by the radius of the array of the external columns R) and the external column diameter D (Li et al., 2024), only both design variables are comprehensive and systematically varied while the others remain with the baseline values. Indeed (Edwards et al., 2024), reported that the semisubmersible draught shows a very weak correlation with wind turbine capacity, having stayed pretty constant

Table 2
Design variables.

Description	Units	Baseline values	Range
Draught, T	m	20.0	–
Radius of external column array, R	m	51.75	30 : 0.1 : 100
External column diameter, D	m	12.5	10 : 0.1 : 20
Central column diameter, d_c	m	10.0	–
Freeboard, f_b	m	15.0	–
Pontoon width	m	12.5	–
Pontoon height	m	7.0	–

around a value of 20 m for most of the designs reported in the literature – which coincidentally is the value adopted in the reference UMaine design. The freeboard also has a minimal impact on initial intact stability (i.e., at small inclinations) although at large inclinations it may have a positive effect on stability by notably increasing the restoring moment and the angle of vanishing stability. Since in the parametric analyses the stability criterion is restricted to angles of 5–10°, freeboard is not expected to play a significant role. Furthermore (Li et al., 2024), found that if stability at large angles is required to be improved, increasing the freeboard implies in twice the amount of material (steel) compared to an alternative increase in external column diameter. Thus, although crucial (especially in survival conditions), the stability at large heeling angles can be considered out of the scope of the preliminary sizing, and should be verified at later design stages using more advanced numerical tools, such as HydroD (DNV, 2024a). Moreover, since freeboard is directly related to green water occurrences, that depend on wave height probability distribution at the offshore site and the corresponding platform motions – which should be computed with higher fidelity numerical tools (at later design stages) –, for the scope of the present work, prescribing a minimum freeboard to avoid green water at representative storm conditions should be enough. The reference UMaine platform adopted a 15 m freeboard for representative sea conditions of the U.S. East Coast with a 50-y significant wave height of 10.70 m – similar to the NE8 offshore site. Thus, the same freeboard is here adopted.

For the sake of comparison and assessment of the results of the parametric analyses, Table 3 displays the main characteristics of the reference UMaine 15-MW platform at the design draught reported in (Allen et al., 2020). Some details of that reference platform are not publicly available, so the Authors have numerically modelled it using the Sesam suite software (DNV, 2024b), proposed a possible compartmentation of the ballast tanks, and performed stability and hydrodynamic analyses for the free-floating condition (including mooring pretension, but without mooring system stiffness). The application of the heeling moment induced by the wind turbine thrust at rated wind speed and the corresponding wind loads on the tower and superstructure on

Table 3
Characteristics of the reference VoltturnUS UMaine 15-MW semisubmersible.

Description	Units	Reference values
Displaced volume	m ³	20206.0
Displaced volume CoB	m	(0.0, 0.0, –13.63)
Hull steel mass (inc. tower interface)	t	4014.0
Hull steel CoG	m	(0.0, 0.0, –14.94)
Ballast mass (fixed/fluid) - permeab. 98%	t	2540/11071
FOWT CoG @ design draught	m	(0.0, 0.0, –1.88)
FOWT inertia wrt CoG	t.m ²	(4.452E+07, 4.459E+07, 2.607E+07)
Transverse metacentric height (GMt) without FSC	m	13.47
Heeling angle @ rated wind speed (free-floating)	deg	8.7
Heave natural period	s	20.5
Roll natural period	s	29.9
Pitch natural period	s	29.9

CoB: Centre of Bouyancy; FSC: Free Surface Correction.

the reference UMaine platform resulted in a static heeling angle of 8.7°, which will be the value adopted as serviceability criterion for our analyses. Although this value may seem close to the upper limit value suggested for serviceability criteria in (DNV, 2021a), it should be noticed that this is a conservative static approach that, among other aspects, neglects the restoring effects of the mooring system.

4. Results and discussion

The first sweep of the design space was performed considering over 70000 floating substructures, defined by the systematic variations of the external column diameter and their array radius (Table 2). Since, the column (centreline) distance is a more practical term than the column array radius, we will use the former to present our results. For semi-submersibles with three uniformly (120°) spaced columns, the column distance is related to the column array radius, R, by:

$$col_{dist} = 2 * R * \sin(\pi / 3) \quad (6)$$

The application of the constraint associated to the intact stability (heeling angle, Θ , induced by the wind inclining moment at rated wind speed), which is expressed as:

$$0.0^\circ < \theta_{@rated_wind}^{stat} \leq 8.7^\circ \quad (7)$$

reduces the design space to 55506 floating substructures for the centred configuration and to 54121 for the off-centred one. Fig. 3 depicts the design space of both semisubmersible designs in terms of the resultant heeling angle, where it is evident that smaller heeling angles represent overconservative solutions with larger floating substructures in terms of external column diameter or column distance. Those solutions certainly penalise the amount of required hull steel mass by moving away from potential optimised cost solutions. On the other hand, the solutions that minimally satisfy the stability criterion, i.e., $\theta_{@rated_wind}^{stat} = 8.7^\circ$, provide smaller floating substructure dimensions and should be the most cost-effective ones. These solutions are located along the black curve highlighted in Fig. 3, and will be further analysed and used for comparison between the off-centred and centred configurations in the following sub-sections.

4.1. Main basic dimensions

Figs. 3 and 4 show that the pairs external column diameter and column-to-column distance are only slightly different between the off-centred and centred configurations in terms of static heeling angle at rated wind speed, especially for the smaller column diameters. These results may preliminarily indicate that the pontoons in the centred configuration hardly contribute to intact stability, and that both semi-submersible designs are comparable in size at waterline level. However, it should be noticed that the off-centred configuration involves heave plates at the column bottoms that protrude beyond the waterline external limits. Indeed, in earlier WindFloat designs, the diameter of the external circumference covered by heave plates was over twice the external column diameter, but in more recent WindFloat designs, heave plate (horizontal) surfaces have been redistributed towards the inner space of the platform, reducing the protuberances extension.

4.2. Bill of material (floating substructure steel mass)

The main objective function in the optimisation of a FOWT platform is cost, which for a preliminary design is typically expressed in terms of bill of material or, utilising a proxy for this, more simply the steel mass required for the floating substructure. This steel mass is computed from the volume of material necessary for the external surfaces of the floating substructure (the hull), i.e., all the surfaces shown in grey in Fig. 2 plus the bracings (for the off-centred configuration), considering a uniform equivalent plate thickness (45.4 mm) and a steel density of 7.85 t/m³.

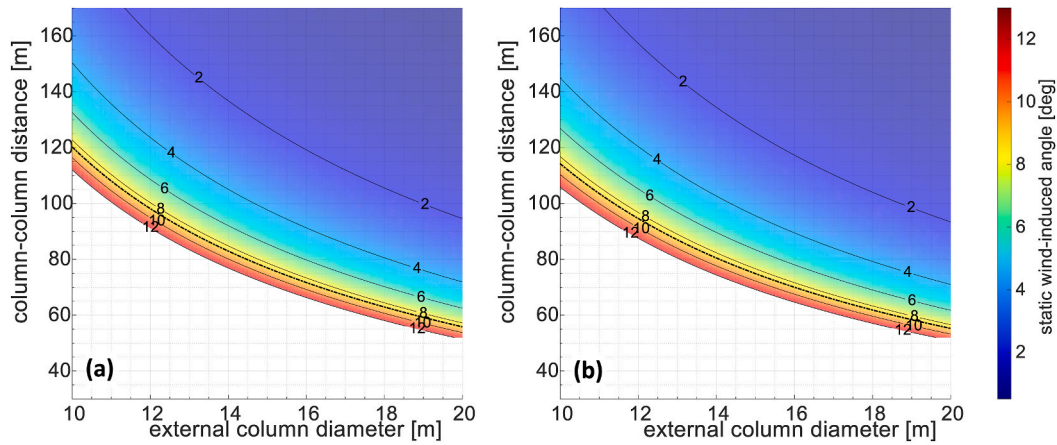


Fig. 3. Design space for semisubmersible configuration: (a) Off-centred (b) Centred.

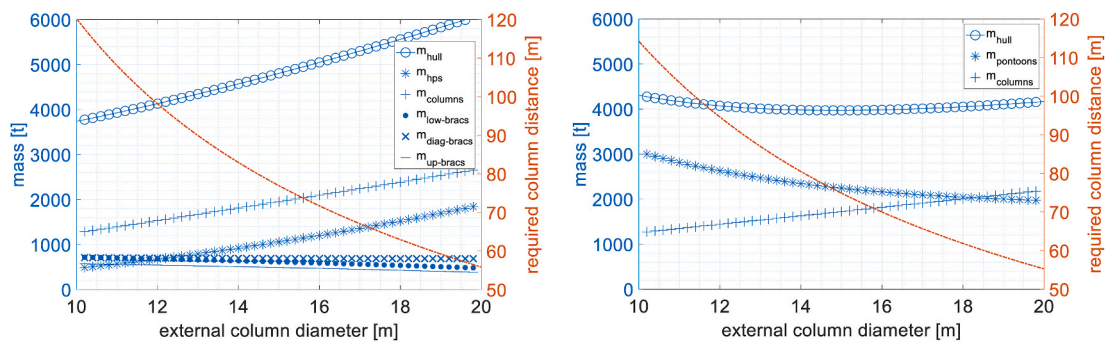


Fig. 4. Floating hull steel mass and main components: (a) Off-centred (b) Centred.

Fig. 4 shows the total steel mass of the floating substructure (m_{hull}) and its main components as function of the column diameter and its associated (required) column distance for the off-centred and centred configurations. The trends and values for the total hull steel mass are significantly different between both designs – despite having comparable external dimensions. Indeed, for the range of investigated column diameters, as the column diameter increases, the mass of the centred configuration follows a concave downwards curve with a minimum of 3971 t at $D = 14.9$ m, while the mass of the off-centred semisubmersible continuously increases surpassing the centred configuration at $D = 11.8$ m. The difference in trends is due to the fact that, for the off-centred configuration, the mass of columns ($m_{columns}$) and heave plates (m_{hps}) are the main contributors, and basically depend on the column diameter. Bracings (lower, diagonal, and upper) play a secondary role, and the increase in their mass with larger column diameters is compensated by the reduction in mass due to their reduced length associated to the smaller column distances. On the other hand, in the centred configuration, pontoons mass ($m_{pontoons}$) represents the major contribution for smaller column diameters, but as column diameter becomes larger (and column distance becomes shorter), this contribution reduces and, at a certain point, is surpassed by the column masses, that mainly depend on column diameter. The growing trend of columns mass and the corresponding reduction in pontoons mass as column diameter increases resulted in the concave mass curve for the centred configuration.

4.3. Equilibrium

The equilibrium analysis is typically considered straightforward and consists in computing the required amount of ballast to achieve a target draught. If the computed ballast mass is greater than zero, it is generally assumed that (even keel) equilibrium is feasible. For designs with

approximately symmetric mass distribution such as the centred configuration, this approach may suffice. However, that assumption does not hold for FOWTs with off-centred configuration. In these cases, achieving equilibrium requires not only a total ballast weight greater than zero, but also an uneven ballast distribution to counterbalance the asymmetrical weight of the tower and RNA: more ballast is required in the (two) columns without the tower and RNA, and less in the other (the one with the tower and RNA) so that the overall centre of gravity is aligned vertically with the at-rest centre of buoyancy. Eventually, the ballast in the tower-supporting column may need to be reduced to a point where “negative ballast” (e.g. buoyancy addition) would be required, which is not feasible in the context of the present study.

To address this, the design constraint associated to a positive value for the total ballast should be extended to specific available compartments within the floating substructure. For preliminary design, global simplified compartmentation can be assumed. For example, in the off-centred configuration, each column is defined as an independent compartment. The tower-supporting column (e.g. col1) will require less ballast due to the additional mass of the tower and RNA, while the other two columns (col2 and col3) receive equal amounts of ballast to maintain transversal equilibrium. In contrast, the centred configuration, with its near symmetric mass distribution, allows for a simple compartmentation scheme. Here, ballast is divided between two major compartments: one for the pontoons (ballast_{pon}) and other for the three external columns (ballast_{col}). The ballast strategy employed in the centred configuration consisted in, first, filling equally only the pontoon compartments. Once the pontoons are full, the column compartments are then equally filled. The central column is not initially considered a ballast compartment, but this could be revisited in later design stages if necessary.

For the present analyses, and aiming at cost reduction, only seawater

was considered as ballast material for both the centred and the off-centred configurations. In reference 15-MW UMaine platform, 2540 t of iron-ore-concrete ballast was used as fixed ballast at the base of the external columns.

The total amount of ballast ($m_{\text{ballast tot}}$) required to achieve the specified draught ($T = 20$ m) as well as the amount of ballast of the major compartments considered for the off-centred and centred configurations are shown in Fig. 5. The total displacement (m_{disp}) and hull steel mass (m_{hull}) of both floating substructures are also presented for comparison purposes.

The analyses of Fig. 5 in terms of the ballast constraint evidence that all centred configurations are satisfactory (all solutions require positive ballast), but for the off-centred configurations, only the floating substructures with $D > 14.6$ m are feasible solutions, i.e., almost half of the current design space for off-centred configurations should be disregarded at this stage. These results may be explained by the much smaller total displacement of off-centred configurations (compared to the corresponding centred ones) associated to less internal volume available for ballast to equilibrate the platform, particularly in col 1, which supports the tower and the RNA. Indeed, if only the constraint related to total ballast is assessed (disregarding the constraint for col1 ballast), all the off-centred configurations with $D > 10.2$ m would have wrongly been judged satisfactory. For the centred configurations, two interesting and relevant aspects deserve further discussion. First, the much larger total displacement may be misleading if associated to the bill of material, because the hull steel mass represents less than 20% of the total displacement, being even less than the hull steel mass of most off-centred configurations. The second aspect is that for centred configurations with $D \leq 12.9$ m, the pontoons volume suffices to satisfy ballast requirements. For larger column diameters, ballast in the columns is required, but the available column volume is enough. Thus, in terms of equilibrium, neither central column ballast nor fixed (solid) ballast is necessary.

4.4. Stability properties

So far, the stability of the off-centred and centred configurations has been assessed only in terms of the inclination angle induced by the wind turbine heeling moment at rated wind speed, as shown in Fig. 3. Although those results indicate that both configurations have comparable performances, due to the striking differences already observed in terms of mass and equilibrium, stability-related properties such as KB, BM, KM, KG, and GM, that govern the static response of the floating platform, are here analysed in detail (Fig. 6).

In terms of stability, semisubmersibles are regarded as waterplane-stabilised floating substructures (Edwards et al., 2023b). Therefore, given that the main waterplane dimensions of the off-centred and centred configurations are similar, in principle, alike values are expected for their stability. However, as evidenced in Fig. 6, significant different patterns are observed between both semisubmersible configurations,

particularly in terms of BM. Although the waterplane second area moment plays a significant role in BM, the displaced volume should not be overlooked. Indeed, the displaced volumes for off-centred configurations are significantly lower than in centred designs, resulting in much higher BMs for the off-centred semisubmersibles than for the centred configurations. Furthermore, in the off-centred semisubmersible, KB is higher than in the centred configuration, because the pontoons volume in the latter pushes KB downwards. In terms of KG, the off-centred semisubmersible has a higher KG than the centred one over the full range of the investigated column diameters. The location and significant contribution of the pontoons in the centred configuration certainly contribute to keeping the KG lower. However, overall, the resultant GM, which represents the initial stability arm of the floating platform, is notably higher for the off-centred semisubmersible than for the centred design. So, how to explain the comparable resulting heeling angles in Fig. 3?

The answer is that the restoring moment (RM) depends not only on the stability arm (which is higher in the off-centred design), but also on the displacement (which is significantly greater in the centred semisubmersible). Then, it turns out that, for centred configuration's restoring moment, the shorter stability arm is compensated by the larger displaced volume. Moreover, for centred semisubmersible, even with smaller GMs, these values are considered satisfactory. Current standards for FOWTs do not specify a minimum GM, so the criterion used for semisubmersible Mobile Offshore Drilling Units – MODUs ($GM \geq 1.0$ m) could be adopted as an indicative value. In that case, for all the potential centred solutions displayed in Fig. 6b, GM ranges from 10.9 m to 13.2 m, i.e., largely satisfy MODUs criterion.

4.5. Hydrodynamic performance: natural periods

Based on the analytical expressions in (DNV, 2021b), the heave added mass and pitch added inertia for the off-centred and centred configurations have been computed and are shown in Fig. 7. The values and trends of both hydrodynamic properties are significantly different for both configurations. In the off-centred design a steady increase in the coefficients is observed as external column diameter increases – consistent with the increase in the size of heave plates (the major contributor). On the other hand, in the centred design, due the larger horizontal area covered, the pontoon is the major contributor in the vertical added mass, depending both on the pontoon width (same as external column diameter) and length (associated to column distance). Thus, while an increase in the column diameter is reflected as an increase in the pontoon width (that favours the increase in added mass), the corresponding reduction in column distance reflects as a decrease in pontoon length (that causes a decrease in added mass). Since the latter reduction is predominant, an overall decrease in added mass and inertia is observed as the column diameter increases.

In Fig. 8, the heave and pitch natural periods for the off-centred and centred configurations are shown. From previous analyses on

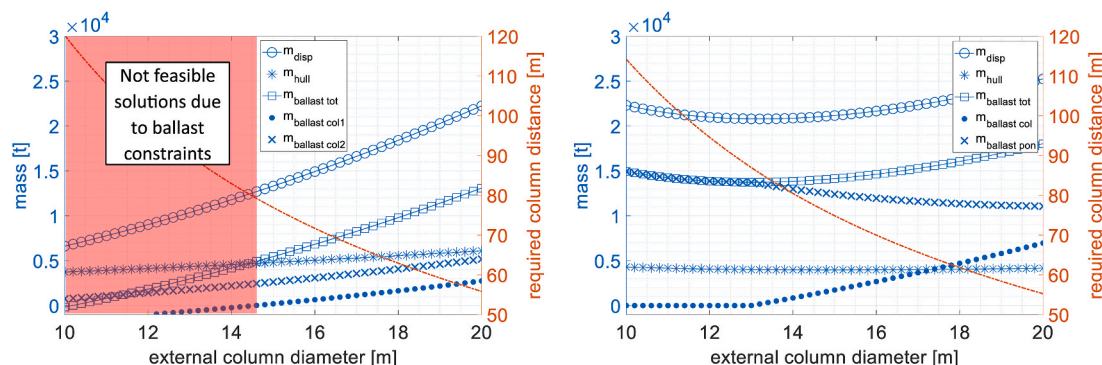


Fig. 5. Overall displacement and ballast required for even keel equilibrium: (a) Off-centred (b) Centred.

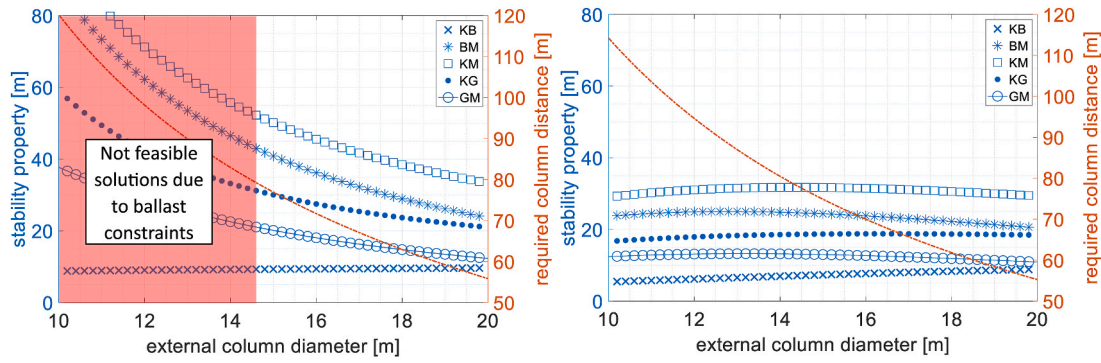


Fig. 6. Stability properties (KB, BM, KM, KG, and GM) at design draught: (a) Off-centred (b) Centred.

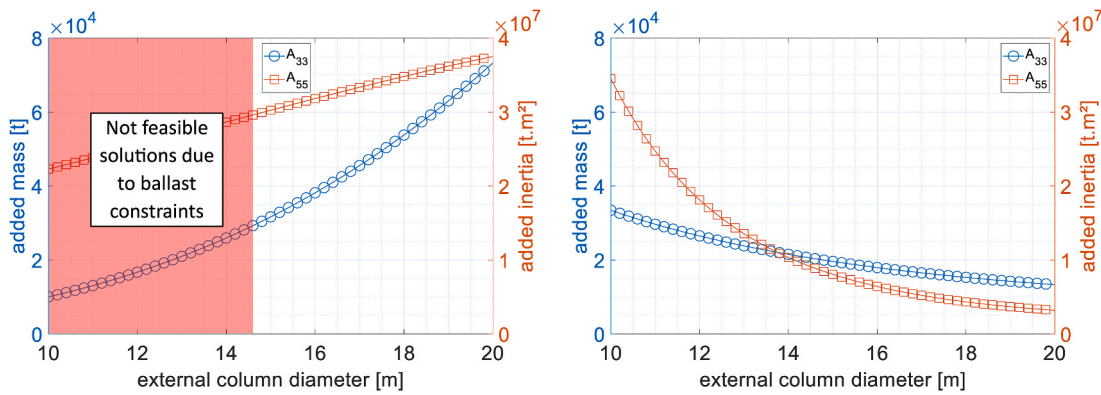


Fig. 7. Added mass in heave and added inertia in pitch: (a) Off-centred (b) Centred.

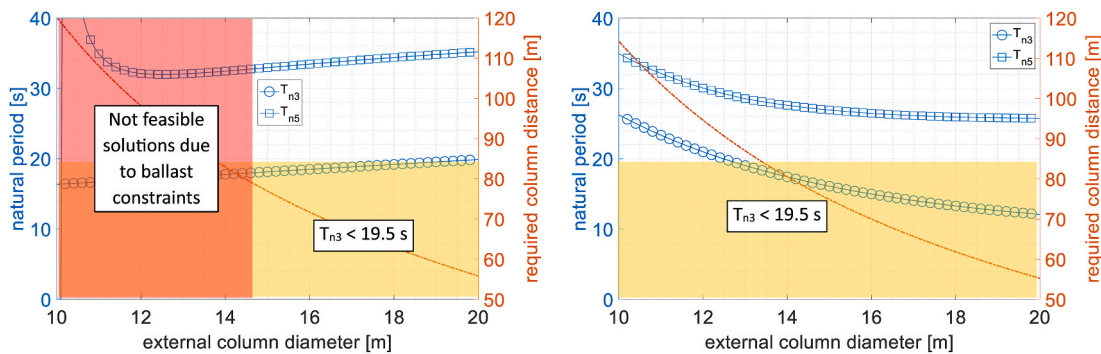


Fig. 8. Uncoupled heave and pitch natural periods at free floating condition: (a) Off-centred (b) Centred.

waterplane dimensions (comparable between both configurations), and the larger displaced volume (and total mass) associated to the centred semisubmersible, in principle, the heave natural periods for this configuration is expected to be larger than the off-centred one – assuming that heave added mass is of the same order of displaced mass (as for most conventional floating substructures). Indeed, that is the case for the centred configuration, where for the investigated range of column diameters, heave added mass ranges between ~ 14000 and ~ 34000 t. However, for the off-centred semisubmersible, due to heave plates, heave added mass ranges from ~ 10000 to 73000 t, i.e., ~ 1 to 3 times its displaced mass, thus with a more significant effect in its heave natural period.

The decrease in heave added mass with the increase in column diameter for centred configurations results in heave natural periods that do not satisfy the typical constraint: $T_{n3} > 17\text{--}20$ s for floating substructures with $D > 14.0$ m. On the other hand, all the (feasible) off-centred configurations satisfy that criterion. Pitch natural period

depends directly on virtual inertia, i.e., the (dry) mass moment of inertia plus hydrodynamic inertia, and inversely on GM. Dry inertia for both designs are comparable due a compensation between the larger displaced mass in centred semisubmersibles and the larger pitch radius of gyration in off-centred semisubmersibles (due to the off-centred location of the tower and RNA). On the other hand, due the significant contribution of the heave plates, the off-centred design has also a much larger added inertia in pitch (A_{55}) that would result in significant larger pitch natural periods than for the centred design. However, since the off-centred configuration's GM is larger than the centred one, the resultant pitch natural periods are somehow compensated by the inversely proportional effect of GM. Nevertheless, the pitch natural periods of both designs still satisfy the typical constraint: $T_{n5} > 20\text{--}25$ s. A more accurate assessment of the suitability of the obtained natural periods and the associated constraints can be performed based on representative sea states of the (given) offshore site. For instance, Fig. 9 displays the 50-y extreme sea spectrum (ESS) and a normal sea state spectrum (NSS) of

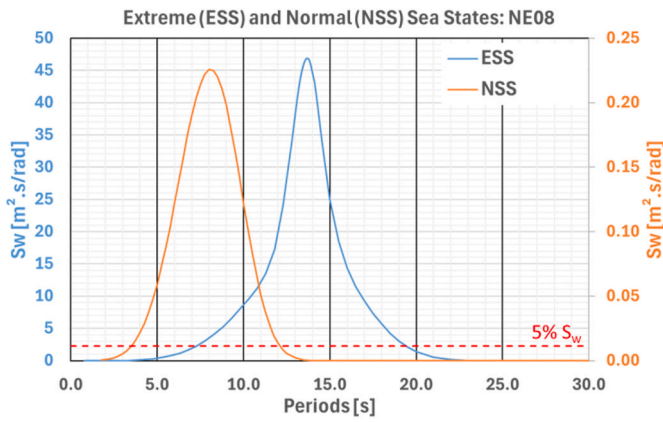


Fig. 9. Sea spectra for two representative sea states of NE8 offshore site.

the offshore site for our case study (the ScotWind area NE8). The NSS is representative of a typical DLC1.3 for an operational condition at a wind speed (at hub level) of 10.59 m/s. The red dashed line shown in that figure represents a threshold of 5% in power density for both sea spectra. This threshold can be used to define the period ranges that the platform's natural periods should avoid regarding resonance. For this case study, it turns out that the ESS is the critical sea state and that $T_{n3}, T_{n5} > 19.5$ s should be a more appropriate constraint to be applied. Therefore, according to Fig. 8, only floating substructures with $D > 18.9$ m for off-centred semisubmersibles or $D < 12.7$ m for centred semisubmersibles would satisfy that criterion for heave natural period – leaving, in principle, a very limited design space for the floating substructure dimensions of both designs. Certainly, the 5 % threshold could be questioned and relaxed to allow for shorter heave natural periods (e.g. $T > 18.0$ s). Under the latter premise, due to the trend of the heave natural period curve for off-centred configurations, its design space would significantly increase allowing for floating substructures with $D > 14.6$ m. On the other hand, the steeper heave natural period curve for centred configurations would just allow a small additional design space with $D < 13.3$ m.

A more advanced approach consists in analysing the wave-induced excitation loads, particularly for relevant borderline floating substructures, i.e., those floating substructures that are judged good or very good from other criteria perspective, but do not satisfy the natural period constraint (but are very close to). Eventually, those floating substructures could be taken forward for more detailed, higher fidelity level analyses at later design stages.

4.6. Hydrodynamic performance: (Froude-Krylov) wave excitation loads

As discussed in previous subsections, in early design stages, the assessment of hydrodynamic performance based on motion response amplitudes may not be reliable, and instead, the prediction of natural

periods was adopted as dimensioning criterion. However, as demonstrated in the case study, the simplified approach based on natural periods could be complemented by an assessment of the wave-induced loads. This assessment can be applied to further reduce the design space or to verify sets of potentially interesting floating substructure solutions that marginally failed to satisfy the natural periods criteria.

Since wave excitation loads are frequency-dependant, here we have assumed that a regular wave with period equal to the peak period of the 50-y sea state (ESS) is representative of the extreme sea state (and the worst wave-induced loads) for the NE8 offshore site. In the context of linear theory, wave height is not meaningful, so that wave excitation loads are computed per unit wave amplitude. Fig. 10 shows the surge and heave (FK) wave-induced forces per unit wave amplitude for both semisubmersible configurations, considering a wave of period $T = 13.71$ s (wavelength, $\lambda = \sim 293$ m), while Fig. 11 depicts pitch (FK) wave-induced moments per unit wave amplitude for the same wave.

Within the range of investigated column diameters for both designs, the off-centred design displays larger heave excitation forces than the centred design, particularly in the region of the smaller column diameters and where heave natural periods are larger than the constraint ($T > 19.5$ s). Indeed, an interesting feature can be observed at $D = \sim 11.2$ m where a cancellation effect took place for the wavelength considered, i.e., a wavelength ~ 3 times the column distance. Comparatively, the centred semisubmersible heave hydrodynamic performance both in terms of natural period and wave-induced force seems better than the off-centred configuration, at least, for the NE8 offshore site. However, in terms of surge wave-excitation loads, the centred semisubmersible underperformed compared to the off-centred semisubmersible, exhibiting (~ 2 – 1.25 times) larger forces over the whole feasible range of off-centred configurations. Those larger surge forces are basically associated to the presence of the pontoons and should be further addressed in mooring system design. Moreover, since this performance corresponds to an extreme sea condition, i.e., survival with wind turbine not in operation, no further implications are expected, except for eventual issues related to the tower. Regarding pitch wave-induced moments, they are expected to play a significant role not only in terms of rigid-body motion responses, but also at a global structural level, especially for ultimate limit state assessment under survival loads. Given that, in terms of pitch natural periods, both designs have shown to be satisfactory, a more accurate (and quantitative) comparative assessment of their performance can be done in terms of the pitch wave excitation moments. Again, over the range of feasible off-centred configurations and for a survival regular wave condition equivalent to ESS, the wave-induced pitch moment for the off-centred design resulted ~ 3 to 2 times larger than for the centred one. Therefore, considering that pitch restoring coefficients for both floating substructures are similar, in a first static approximation (long waves), the wave-induced pitch motion response amplitudes under survival conditions are expected to be also ~ 3 to 2 times larger in the off-centred than in the centred semisubmersible.

It should be mentioned that for the sake of simplicity, in our case

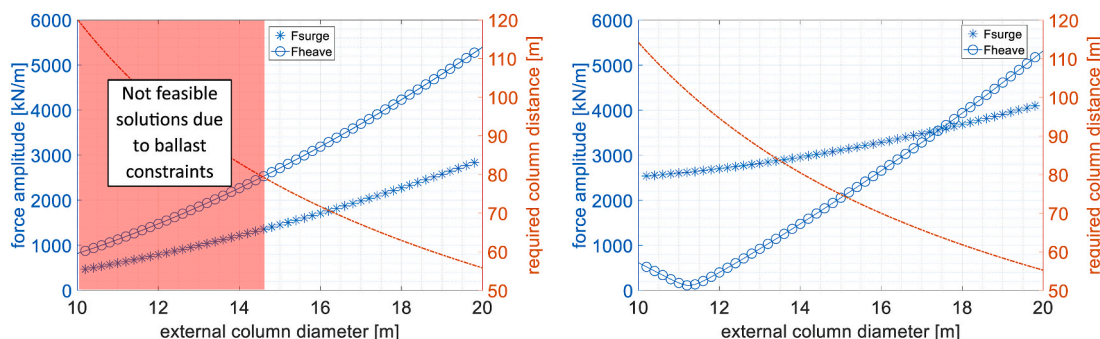


Fig. 10. FK surge and heave forces per unit wave amplitude for a wave of $\lambda = \sim 293$ m, $\beta = 0^\circ$: (a) Off-centred (b) Centred.

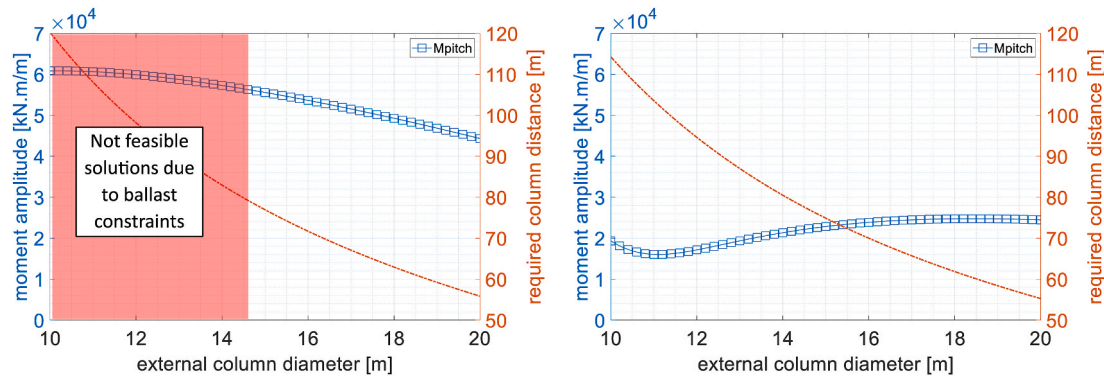


Fig. 11. FK pitch moment per unit wave amplitude for a wave of $\lambda = \sim 293$ m, $\beta = 0^\circ$:(a) Off-centred (b) Centred.

study, the computation of wave-induced loads on the bracings of off-centred semisubmersible have not been considered. Indeed, due to the characteristic dimensions of those members (much smaller diameter than columns), they are usually not included in panel methods modelling but are described as Morison elements. Their effect is expected to be negligible on wave-induced loads, but if perceptible, they would have accentuated the differences between off-centred and centred configurations.

4.7. Comparison summary and potential best solutions

Based on the results and discussions of previous subsections, some of the most meaningful outputs for both floating substructures have been selected and summarised in Table 4. The potential floating substructure solutions are displayed in terms of pairs (column diameter, column spacing) that beforehand have minimally satisfied the wind heeling angle criterion, $\theta_{\text{rated_wind}}^{\text{stat}} = 8.7^\circ$. Within these solutions, a few that have severely violated ballast or natural period criteria have been left as references (grey cells). To aid in the assessment, colour scale (green-orange-red) formatting has been adopted for the hull mass values of each semisubmersible configuration, where green identifies the least, orange the intermediate and red the greatest values.

The monotonic (either increasing or decreasing) trends exhibited by most off-centred design's outputs, and the constraint $D \geq 14.6$ m imposed by the feasibility criteria related to ballast capacity inside the column that holds the (off-centred) tower (and RNA), allows the identification of basically three potential floating substructure solutions:

- a) $D = 14.6$ m, $\text{col}_{\text{dist}} = 79.0$ m. This solution performs the best in most analysed criteria with the least hull steel mass (4711 t) among the

feasible ones, but it (marginally) fails to satisfy the heave natural period criterion.

- b) $D = 18.9$ m, $\text{col}_{\text{dist}} = 60.0$ m. This solution minimally satisfies all the criteria, but its hull steel mass is 5802 t, i.e., 23% higher than solution a).
- c) $D = 20.0$ m, $\text{col}_{\text{dist}} = 56.0$ m. This solution satisfies all the criteria and, additionally, has the lowest pitch wave-induced moment, however its hull mass is 6306 t, i.e., 34 % higher than solution a).

Although solution (a) (marginally) fails the natural heave criterion, its superior performance in the other outputs, particularly in terms of hull steel mass (i.e., bill of material), makes this solution relevant for further analyses. If the fulfilment of the heave natural period criterion for the NE8 offshore site ($T_{n3} \geq 19.5$ s) is enforced, the design space would be reduced to floating substructures with $D \geq 18.9$ m (see Fig. 8). Indeed, the alternative solutions (b) and (c) satisfy all the criteria, but both result in considerably larger hull steel mass (i.e., cost) compared to solution a). Certainly, at the detailed design stage, where all loads are accounted for the determination of hull thickness and scantlings, hull steel mass will be more accurately estimated, but the relative tendencies observed here are expected not to change significantly. Therefore, solution a) should still be considered as a potential (best) solution, provided that, in later design stages, the heave motion amplitudes for extreme sea states (ESS) prove to be within acceptable limits.

Unlike the off-centred semisubmersible, the centred semisubmersible displays more generic trends for most output parameters, offering also a larger feasible design space. In general, there is a different floating substructure solution that best satisfy each output considered, except for the lowest natural period case (highlighted in grey in Table 4) where the solution falls completely within the more energetic range of wave periods for the ESS. Nevertheless, like the off-centred

Table 4
Summary of meaningful outputs for the off-centred and centred configurations.

Output	Off-centred semisub				Centred semisub			
	Value	D [m]	Col _{dist} [m]	Hull mass [t]	Value	D [m]	Col _{dist} [m]	Hull mass [t]
Least hull steel mass (t)	3738.8	10.0	120	3739	3971.0	14.9	75	3971
Least total ballast (t)	20.6	10.2	118	3776	13734.5	13.0	87	4011
Least cmptm ballast (t)	23.8	14.6	79	4711	9.7	13.0	87	4011
Least displacement (t)	12703.0	14.6	79	4711	20809.9	13.0	87	4011
Largest KM	52.2	14.6	79	4711	31.7	14.4	78	3973
Lowest KG	21.0	20.0	56	6106	16.6	10.0	114	4306
Largest GM	21.0	14.6	79	4711	13.2	13.2	86	4002
Lowest T_{n3}	18.0	14.6	79	4711	12.1	20.0	55	4168
Lowest T_{n3} (suitable)	19.5	18.9	60	5802	19.6	12.7	89	4026
Highest T_{n3}	19.9	20.0	56	6106	26.3	10.0	114	4306
Lowest T_{n5}	32.7	14.6	79	4711	25.8	20.0	55	4168
Highest T_{n5}	35.2	20.0	56	6106	35.0	10.0	55	4306
Lowest Fsurge	1359.0	14.6	79	4711	2528.6	10.0	55	4306
Lowest Fheave	2533.0	14.6	79	4711	113.2	11.3	101	4134
Lowest Mpitch	44318.4	20.0	56	6106	16018.3	11.1	103	4156

configuration, if the heave natural period criterion for NE8 site is enforced (see Fig. 8), the centred configuration design space can be significantly constrained to only floating substructure options with $D \leq 12.7$ m. Even in that case, there are still some suitable good options in terms of lowest excitation loads or natural periods that can be considered without a significant increase in bill of material, such as the floating substructure with the lowest wave-induced pitch moment ($D = 11.1$ m and $col_{dist} = 103$ m) that require a hull steel mass of 4156 t, i.e., 5% higher than solution with the least hull steel mass. The floating substructure solution $D = 12.7$ m and $col_{dist} = 89$ m minimally satisfies the heave natural period criterion with a hull steel mass of 4026 t, i.e., only 1.4% higher than the solution with the least hull steel mass).

The best suitable solutions for both designs could be summarised as follows:

Off-centred: $D = 18.9$ m, $col_{dist} = 60$ m with $m_{hull} = 5802$ t

Centred: $D = 12.7$ m, $col_{dist} = 89$ m with $m_{hull} = 4026$ t

The off-centred solution $D = 14.6$ m, $col_{dist} = 79$ m with $m_{hull} = 4711$ t could be considered also a potential solution but requires further assessment of its heave motion responses for NE8's ESS. The UMaine best solution obtained here is pretty similar to reference 15-MW UMaine floating substructure ($D = 12.5$ m, $col_{dist} = 89.6$ m with $m_{hull} = 4014$ t), but has a slightly smaller GM (13.2 m) compared to reference's GM (13.5 m). That difference is due to the lower KG, resulting from the (solid) fixed ballast adopted in the reference design. In terms of heave and pitch natural periods the differences may be deemed negligible.

Since the scope of this work is the early design stage of the floating substructure, some relevant aspects of the FOWT system, which demand two-way interactions among the component subsystems (tower, RNA, servocontrol, mooring system, export cable) have been simplified by considering only their effect on the substructure and not the other way around (and their potential feedback). For instance, the floating substructure characteristics strongly determine the tower design and dictates the tower bending modes, which influence the FOWT dynamic performance. Although those aspects are essential for the FOWT design and could be incorporated in early design stage, they are expected not to have a disruptive effect in the preliminary sizing of the floating substructure – provided that the initial guess of the input data (for instance, the tower design), is reasonable.

5. Conclusions

The exploration and analyses of the design space for off-centred and centred semisubmersible configurations provide valuable insights into the development of high-capacity floating offshore wind turbines (FOWTs). Represented by the off-centred and centred semisubmersible configurations, these two design philosophies highlight critical differences and challenges in scaling FOWTs for turbine capacities of 15 MW and beyond. Both configurations share a common arrangement of three external columns but differ significantly in tower placement and structural components. The off-centred configuration features an off-centred tower with bracings and heave plates, while the centred configuration employs a centred tower supported by a dedicated (central) column and its attached pontoons.

This study systematically evaluated and compared these configurations to address key challenges in the design and scaling of FOWTs. Building upon the foundational designs of off-centred and centred semisubmersibles, the work adopted a global design methodology as outlined by (Li et al., 2024). A parameterised approach was employed for both semisubmersible configurations, integrating free and derived design variables, to systematically determine floating substructure dimensions, mass properties, equilibrium, stability, natural periods, and wave-induced loads. The findings underscore the strengths and trade-offs between centred and off-centred tower configurations:

- **Floating substructure dimensions:** Both designs require comparable column diameters and spacings to meet similar stability criteria.
- **Steel mass:** The centred configuration requires significantly less hull steel mass than the off-centred design, for equivalent waterplane dimensions.
- **Ballast constraints:** The off-centred semisubmersible introduces strict ballast distribution requirements, significantly limiting the feasible design space, whereas the centred configuration allows greater design flexibility.
- **Stability characteristics:** While the off-centred design has a greater intact stability arm, both designs achieve comparable pitch restoring moments due to the centred configuration's larger displacement.
- **Natural periods:** The off-centred configuration faces limitations in increasing heave added mass due its already large heave plates, whereas the centred configuration potentially offer alternative solutions to address natural period constraints.
- **Wave Loads:** The off-centred semisubmersible experiences significantly higher heave and pitch wave-induced loads under extreme sea states, while the centred semisubmersible demonstrates lower sensitivity to these forces.

This study highlights the broader implications of tower placement on FOWT design. The centred configuration offers significant advantages in terms of mass efficiency, design flexibility, and load performance, making it a compelling option for large-scale deployment.

5.1. Contributions and novelty

- This work provides a systematic comparison of centred and off-centred semisubmersible configurations, using two representative designs as case studies.
- The proposed methodology, grounded in fundamental naval architecture principles, offers a computationally efficient alternative to more resource-intensive approaches, making it well-suited for exploring large design spaces.
- The application of the Froude-Krylov approach in preliminary design stages demonstrates its utility for assessing extreme sea conditions and its potential for integration into global structural design analyses.

By advancing the understanding of the design trade-offs between centred and off-centred semisubmersible configurations, this research contributes to refining proven FOWT concepts, supporting the development of efficient and scalable floating wind energy systems, and accelerating the transition to ocean renewables.

CRedit authorship contribution statement

Claudio A. Rodríguez Castillo: Writing – review & editing, Writing – original draft, Software, Methodology, Investigation, Formal analysis, Data curation, Conceptualization. **Maurizio Collu:** Writing – review & editing, Supervision, Investigation. **Feargal Brennan:** Supervision, Project administration, Funding acquisition.

Declaration of competing interest

The authors declare that they have no known competing financial interests or personal relationships that could have appeared to influence the work reported in this paper.

Acknowledgments

This work was funded by the UK Engineering and Physical Sciences Research Council (EPSRC) as part of the Ocean-REFuel (Ocean Renewable Energy Fuels) Programme Grant EP/W005212/1 awarded to the

University of Strathclyde, Newcastle University, University of Nottingham, Cardiff University, and Imperial College London.

Appendix A. Supplementary data

Supplementary data to this article can be found online at <https://doi.org/10.1016/j.oceaneng.2025.120740>.

References

- ABS, 2021. Floating Offshore Wind Turbine Development Assessment. ABS Group Consulting Inc. Report N° Arlington, VA - USA. <https://www.boem.gov/sites/default/files/documents/renewable-energy/studies/Study-Number-Deliverable-4-Final-Report-Technical-Summary.pdf>
- Allen, C., Viscelli, A., Dagher, H., Goupee, A., Gaertner, E., Abbas, N., Hall, M., Barter, G., 2020. Definition of the UMaine VoltturnUS-S Reference Platform Developed for the IEA Wind 15-Megawatt Offshore Reference Wind Turbine. University of Maine, National Renewable Energy Laboratory (NREL). Report N°. <https://www.nrel.gov/docs/fy20osti/76773.pdf>.
- Banister, K., 2017. WindFloat Pacific Project, Final Scientific and Technical Report. Principle Power, Inc., Emeryville, CA (United States) <https://doi.org/10.2172/1339449>. Report N° DE-EE0005987.
- BT. BT Floater Design, 2024. Bassoe technology. <https://www.basstech.se/17/11/renewables/>. (Accessed 26 October 2024).
- Castro-Santos, L., Diaz-Casas, V., 2014. Life-cycle cost analysis of floating offshore wind farms. *Renew. Energy* 66, 41–48. <https://doi.org/10.1016/j.renene.2013.12.002>.
- Cermelli, C., Roddier, D., Aubault, A., 2009. WindFloat: a floating foundation for offshore wind turbines—Part II: hydrodynamics analysis. ASME 2009 28th international conference on ocean, offshore and arctic engineering volume 4. *Ocean Eng.; Ocean Renew. Energy; Ocean Space Utilization, Parts A and B* 135–143. <https://doi.org/10.1115/OMAE2009-79231>.
- Crown-State-Scotland, 2021. ScotWind Leasing: Seabed Leasing for New Offshore Wind Farms. Crown Estate Scotland. Report N° Edinburgh. <https://www.crownstatescotland.com/sites/default/files/2023-07/scotwind-leasing-offer-document-april-2021.pdf>.
- DNV, 2021a. Coupled Analysis of Floating Wind Turbines. Recommended Practice, DNV-RP-0286.
- DNV, 2021b. Environmental Conditions and Environmental Loads. Recommended Practice. DNV-RP-C205.
- DNV, 2024a. Hydrodynamic analysis and stability analysis solver - HydroD. <https://www.dnv.com/services/hydrodynamic-analysis-and-stability-analysis-software-hydrod-14492/>. (Accessed 13 September 2024).
- DNV, 2024b. Sesam Modules for Floating OWT Structures. Det Norske Veritas. <https://www.dnv.com/services/sesam-modules-for-floating-owt-structures-89995/>. (Accessed 6 October 2024).
- Dos Santos, C.R., Stenbro, R., Stieng, L.E., Hanseen-Bauer, Ø.W., Wendt, F., Psychogios, N., Aardal, A.B., 2024. Active control of yaw drift of single-point moored wind turbines. *J. Phys. Conf.* 2767 (3), 032014. <https://doi.org/10.1088/1742-6596/2767/3/032014>.
- Edwards, E., Holcombe, A., Brown, S., Ransley, E., Hann, M., Greaves, D., 2023a. Supplementary information on early-stage floating offshore wind platform designs. United Kingdom. <https://doi.org/10.24382/scvw-0t77>.
- Edwards, E.C., Holcombe, A., Brown, S., Ransley, E., Hann, M., Greaves, D., 2023b. Evolution of floating offshore wind platforms: a review of at-sea devices. *Renew. Sustain. Energy Rev.* 183, 113416. <https://doi.org/10.1016/j.rser.2023.113416>.
- Edwards, E.C., Holcombe, A., Brown, S., Ransley, E., Hann, M., Greaves, D., 2024. Trends in floating offshore wind platforms: a review of early-stage devices. *Renew. Sustain. Energy Rev.* 193, 114271. <https://doi.org/10.1016/j.rser.2023.114271>.
- Equinor, 2024. Hywind Tampen: the world's first renewable power for offshore oil and gas. <https://www.equinor.com/energy/hywind-tampen>. (Accessed 5 October 2024).
- Fenu, B., Attanasio, V., Casalone, P., Novo, R., Cervelli, G., Bonfanti, M., Sirigu, S.A., Bracco, G., Mattiazzo, G., 2020. Analysis of a gyroscopic-stabilized floating offshore hybrid wind-wave platform. *J. Mar. Sci. Eng.* 8 (6), 439. <https://doi.org/10.3390/jmse8060439>.
- Ferri, G., Marino, E., Bruschi, N., Borri, C., 2022. Platform and mooring system optimization of a 10 MW semisubmersible offshore wind turbine. *Renew. Energy* 182, 1152–1170. <https://doi.org/10.1016/j.renene.2021.10.060>.
- Flotation-Energy, 2024. Kincardine – once the world's largest floating wind project. <https://flotationenergy.com/kincardine-once-the-worlds-largest-floating-wind-project/>. (Accessed 5 October 2024).
- Fred Olsen 1848, 2024. The floating foundation BRUNEL, fed. Olsen 1848 AS. <https://www.fredolsen1848.com/floating-wind/brunel/>. (Accessed 26 October 2024).
- Gaertner, E., Rinker, J., Sethuraman, L., Zahle, F., Anderson, B., Barter, G.E., Abbas, N.J., Meng, F., Bortolotti, P., Skrzypinski, W., 2020. IEA Wind TCP Task 37: Definition of the IEA 15-megawatt Offshore Reference Wind Turbine. National Renewable Energy Lab.(NREL), Golden, CO (United States). Report N°. <https://www.nrel.gov/docs/fy20osti/75698.pdf>.
- Ghigo, A., Cottura, L., Caradonna, R., Bracco, G., Mattiazzo, G., 2020. Platform optimization and cost analysis in a floating offshore wind farm. *J. Mar. Sci. Eng.* 8 (11), 835. <https://doi.org/10.3390/jmse8110835>.
- Hersbach, H., Bell, B., Berrisford, P., Biavati, G., Horányi, A., Muñoz Sabater, J., Nicolas, J., Peubey, C., Radu, R., Rozum, I., Schepers, D., Simmons, A., Soci, C., Dee, D., Thépaut, J.-N., 2023. ERA5 hourly data on single levels from 1940 to present. Copernicus Climate Change Service (C3S). <https://cds.climate.copernicus.eu/cdsapp#!/dataset/reanalysis-era5-single-levels?tab=overview>. (Accessed 17 September 2024).
- Karimi, M., Hall, M., Buckham, B., Crawford, C., 2017. A multi-objective design optimization approach for floating offshore wind turbine support structures. *J. Ocean Eng. Marine Energy* 3, 1–19. <https://doi.org/10.1007/s40722-016-0072-4>.
- Lee, C., Newman, J., 2013. WAMIT user manual, version 7.0. Report N°. <https://www.wamit.com/manual.htm>.
- Lemmer, F., Yu, W., Müller, K., Cheng, P.W., 2020. Semi-submersible wind turbine hull shape design for a favorable system response behavior. *Mar. Struct.* 71, 102725. <https://doi.org/10.1016/j.marstruc.2020.102725>.
- Lewis, E.V., 1988. Principles of Naval Architecture. Vol. I – Stability and Strength. The Society of Naval Architects and Marine Engineers (SNAME). ISBN No. 0-939773-00-7.
- Li, C., Zhou, S., Shan, B., Hu, G., Song, X., Liu, Y., Hu, Y., Yiqing, X., 2022. Dynamics of a Y-shaped semi-submersible floating wind turbine: a comparison of concrete and steel support structures. *Ships Offshore Struct.* 17 (8), 1663–1683. <https://doi.org/10.1080/17445302.2021.1937801>.
- Li, W., Wang, S., Moan, T., Gao, Z., Gao, S., 2024. Global design methodology for semi-submersible hulls of floating wind turbines. *Renew. Energy* 225, 120291. <https://doi.org/10.1016/j.renene.2024.120291>.
- Luan, C., 2018. Design and Analysis for a Steel Braceless Semi-submersible Hull for Supporting a 5-MW Horizontal axis Wind Turbine. Norwegian University of Science and Technology, Trondheim. <http://hdl.handle.net/11250/2563372>.
- Mahfouz, M.Y., Molins, C., Trubart, P., Hernández, S., Vigara, F., Pegalajar-Jurado, A., Bredmose, H., Salari, M., 2021. Response of the international energy agency (IEA) wind 15 MW WindCrete and activefloat floating wind turbines to wind and second-order waves. *Wind Energy Sci.* 6 (3), 867–883. <https://doi.org/10.5194/wes-6-867-2021>.
- Mareal, XCF, 2024. Mareal. <https://www.mareal.eu/en/research-and-development/xcf>. (Accessed 26 October 2024).
- Matsuoka, R., Takeda, T., Kusumoto, H., Kuwada, S., Yoshimoto, H., Kamizawa, K., 2022. Development of 12MW cross-shaped semi-submersible floating offshore wind turbine. ASME 2022 41st International Conference on Ocean, Offshore and Arctic Engineering Volume 8: Ocean Renewable Energy. <https://doi.org/10.1115/OMAE2022-79432>.
- NOV, 2024. Tri-Floater Floating Offshore Wind Turbine Foundation. GustoMSC. <https://www.nov.com/products/tri-floater-floating-offshore-wind-turbine-foundation>. (Accessed 26 October 2024). odjell-oceanwind, Deepsea Star™, odjell oceanwind. <https://odjelloceanwind.com/deepsea-startm/>; 2024.
- Ojo, A., Collu, M., Coraddu, A., 2022. Multidisciplinary design analysis and optimization of floating offshore wind turbine substructures: a review. *Ocean Eng.* 266, 112727. <https://doi.org/10.1016/j.oceaneng.2022.112727>.
- Patryniak, K., Collu, M., Coraddu, A., 2022. Multidisciplinary design analysis and optimisation frameworks for floating offshore wind turbines: state of the art. *Ocean Eng.* 251, 111002. <https://doi.org/10.1016/j.oceaneng.2022.111002>.
- Principle-Power, 2024. The WindFloat® advantage installation: ready, set, tow!, principle power. <https://www.principlepower.com/windfloat/advantage/insallation>. (Accessed 1 November 2024).
- Principle. WindFloat Pacific OSW Project, 2014. Report N° Sacramento, CA - United States. <https://www.boem.gov/sites/default/files/about-boem/BOEM-Regions/Pacific-Region/Renewable-Energy/11-Kevin-Bannister-BOEM-Workshop.pdf>.
- Proskovics, R., 2018. Floating offshore wind: a situational analysis. ORE Catapult; Report N° AP-0017. <https://cms.ore.catapult.org.uk/wp-content/uploads/2018/10/Floatin-g-Offshore-Wind-A-Situational-Analysis-Roberts-Proskovics-ORE-Catapult-1.pdf>.
- Robertson, A., Jonkman, J., Masciola, M., Song, H., Goupee, A.A.C., Luan, C., 2014. Definition of the semisubmersible floating system for phase II of OC4. NREL Technical Report. Report N° NREL/TP-5000-60601. <https://www.nrel.gov/docs/fy14osti/60601.pdf>. doi:10.2172/1155123.
- Roddier, D., Cermelli, C., Aubault, A., Peiffer, A., 2017. Summary and conclusions of the full life-cycle of the WindFloat FOWT prototype project. ASME 2017 36th International Conference on Ocean, Offshore and Arctic Engineering Volume 9: Offshore Geotechnics; Torger Moan Honoring Symposium. <https://doi.org/10.1115/OMAE2017-62561>.
- Silva de Souza, C.E., Berthelsen, P.A., Eliassen, L., Bachynski, E.E., Engebretsen, E., Haslum, H., 2021. Definition of the INO WINDMOOR 12 MW base case floating wind turbine. SINTEF Ocean; Report N° OC2020 A-044. Norway. <https://hdl.handle.net/11250/2723188>.
- Sykes, V., Collu, M., Coraddu, A., 2023. A review and analysis of optimisation techniques applied to floating offshore wind platforms. *Ocean Eng.* 285, 115247. <https://doi.org/10.1016/j.oceaneng.2023.115247>.
- Trivane, 2022. Trivane - floating offshore wind (FOW) platform: a semi-submersible turret-moored trimaran Trivane. <https://www.trivaneldt.com/>. (Accessed 26 October 2024).
- Viselli, A.M., Goupee, A.J., Dagher, H.J., Allen, C.K., 2016. Design and model confirmation of the intermediate scale VoltturnUS floating wind turbine subjected to its extreme design conditions offshore Maine. *Wind Energy* 19 (6), 1161–1177. <https://doi.org/10.1002/we.1886>.

- Wayman, E.N., 2006. Coupled Dynamics and Economic Analysis of Floating Wind Turbine Systems. Massachusetts Institute of Technology. <http://hdl.handle.net/1721.1/35650>.
- Yang, H.-S., Alkhabbaz, A., Edirisinghe, D.S., Tongphong, W., Lee, Y.-H., 2022. FOWT stability study according to number of columns considering amount of materials used. *Energies* 15 (5). <https://doi.org/10.3390/en15051653>.
- Zhou, S., Li, C., Xiao, Y., Wang, X., Xiang, W., Sun, Q., 2023. Evaluation of floating wind turbine substructure designs by using long-term dynamic optimization. *Appl. Energy* 352, 121941. <https://doi.org/10.1016/j.apenergy.2023.121941>.